# A Numerical Investigation of The Energy Transfer of A Body Under Fluidelastic Galloping

By H.G.K.G Jayatunga

A thesis submitted to Monash University in fulfilment of the requirements for the Degree of

## Doctor of Philosophy

Department of Mechanical Engineering
Monash University
October 2015

# Statement of originality

This thesis contains no material that has been accepted for the award of a degree or diploma in this, or any other, university. To the best of the candidates knowledge and belief, this thesis contains no material previously published or written by another person except where due reference is made in the text.

Kasun Gayantha Jayatunga

October 2015

# Abstract

The potential of energy harvesting through fluid-elastic galloping is explored through studying the energy transfer between the body and the fluid. This study identified a need for new scaling parameters to better represent fluid-elastic galloping as the parameters used currently (i.e. the traditional Vortex Induced Vibration parameters) were not providing a satisfactory collapse. After reviewing earlier works, this study proposed and tested a hypothesis which assets that delaying the shear layer reattachment would lead to a higher power output. To meet the identified requirements, this study was divided into two main phases. Phase one aims to study the underpinning mechanical parameters while phase two was to understand the fluid mechanics of the system and attempt to control the fluid flow to gain a higher power output.

This fundamental study is carried out using theoretical modelling and numerical simulations. The Quasi-Steady State (QSS) model and Direct Numerical Simulations (DNS) on both stationary and oscillatory cases are carried out to obtain the data.

Phase 1 was initiated by formulating new governing non-dimensional parameters for galloping namely, the combined mass-stiffness, $\Pi_1$ and the combined mass-damping $\Pi_2$. These parameters were formulated using the natural time scales of the linearised QSS equation. The formulated dimensionless groups provided a good collapse for the predicted power output in comparison with the classical VIV parameters which have been traditionally used, i.e. $U^*$, $m^*$, and $\zeta$, reinforcing the statement of Païdoussis et al. (2010) that galloping is a "velocity dependent damping controlled" system. A comparison between the quasi-steady state and direct numerical simulation data, revealed that the quasi-steady state model provides a good approximation of the power output at high $\Pi_1$. However, the QSS approximation deviates from the DNS predictions at low values of $\Pi_1$ because the QSS model does not model vortex shedding which becomes more significant as $\Pi_1$ decreases. Be

that as it may, the QSS model does provide a reasonable prediction of the value of $\Pi_2$ at which maximum power is produced. Both the error in predicted maximum power between the QSS and the DNS models and the relative power of the vortex shedding have been quantified and scale approximately to $1/\sqrt{\Pi_1}$ .

To completely describe the system in terms of $\Pi_1$ and $\Pi_2$, a frequency study was carried out. An expression for the frequency based on $\Pi_1$ and $\Pi_2$ was formulated. This expression was formulated using the eigenvalues of the linearised QSS model and hence was termed the linear frequency, $f_{lin}$. Two regions of frequency response were identified namely, the region where a linear frequency is predicted and the region where $f_{lin}$ does not exist. Both frequency data obtained using QSS model and DNS agreed well with $f_{lin}$ within the boundaries of the DNS simulations conducted, where lower boundary of $\Pi_1$ was limited to $\Pi_1 = 10$ because the galloping signal got weaker when $\Pi_1 < 10$.

QSS frequency was scaled with the undamped natural frequency of the system $f$, in the region where a $f_{lin}$ could not be defined. This revealed that it was within $0.55 \leq \frac{f_{QSS}}{f} \leq 0.75$ in the rage of $0.06 \leq \Pi_1 \leq 0.1$ and dropped further as $\Pi_1$ reduces.

The mere existence of this region is questionable as no DNS data could be obtained in this region due to the fact that galloping signal was weak and the techniques used to obtain the frequency was not sensitive enough to capture the weak signals. There is scope for further study to corroborate or otherwise the QSS prediction using experiments or DNS.

Be that as it may, The linear expression provided a excellent prediction within the boundaries of data obtained through DNS and therefore confirming that frequency predicted by linearised oscillator model expressed in $\Pi_1$ and $\Pi_2$ is accurate.

The second phase of this study initiated by testing the hypothesis of gaining higher power output by delaying the flow re-attachment. In order to investigate test this, a square cross section was systematically tapered off from the top and bottom of the cross section.

A negative region of the $C_y$vs. $\theta$ curve beyond $\frac{d}{l} \leq 0.25$ could be observed in this study. Therefore, as a consequence, there is a loss of power in a certain portion of the galloping cycle which is a result of the velocity and the transverse forcing $F_y$ being out of phase.

The maximum mean power increases as $\frac{d}{l}$ is degreased until $\frac{d}{l} = 0.25$. However, further analysis revealed that the maximum power at $\frac{d}{l} = 0.25$ was grater than $\frac{d}{l} = 0$ which was found out to be a direct result of the size of the negative region of the $C_y$ vs. $\theta$ curve.

Further investigation of the surface pressure data and the velocity magnitude data revealed that the initial negative region was created as a result of the uneven flow distribution due to the profile and the positioning of the geometry, which generated $C_y$ similar to the generation of lift of an aerofoil. As the incidence angle was further increased this mechanism was suppressed by the force created due to the relative proximity of shear layers to the wall, which is typically associated with the positive region of the $C_y$vs. $\theta$ curve.

Comparison of QSS maximum power data and FSI data provided similar trends of maximum power being increased as $\frac{d}{l}$ was decreased proving the initial hypothesis. However, the difference between the QSS and FSI maximum power data increased exponentially as $\frac{d}{l}$ reduced. Investigations carried out using time averaged flow-filed data concluded that the mean flow of the FSI simulations had a significant deviation with the corresponding stationary DNS data. This was a result of the incurred higher traverse velocities as $\frac{d}{l}$ was decreased. As a result significant non-linear forcing was present, which resulted in a deviation from the quasi-steady assumption. Be that as it may, as concluded in phase one of this study, the QSS model could be used as a tool to obtain initial qualitative approximations to design galloping energy harvesting systems.

Obtaining a good balance between the negative and the positive regions of the of the $C_y$ vs. $\theta$ curve is a key design consideration in obtaining an optimum cross section for energy harvesting purposes. Although delaying the shear layer reattachment has it's advantages, the negative region of the $C_y$ vs. $\theta$ curve has an adverse effect on power transfer.

One of the areas for research in future is investigating ways to reduce the negative region of the $C_y$ curve by making alterations to the geometry. Changing the proximity of the shear layers by rounding the edges of the separation points could be one possible approach which can be investigated as future research.

# Acknowledgments

I would like to express my deepest gratitude to my supervisors, Dr. Tan Boon Thong (Dr. Kenny) and Dr Justin Scott Leontini. Dr. Kenny thank you for entertaining me when I was having difficulties. Dr Justin, for explaining me complicated concepts and helping, guiding and providing words of encouragement when I was going through tough situations. I would like to thank both my supervisors for training me to conduct quality research and teaching me proper research techniques.

My warmest gratitude goes to the administrator of the Monash High-performance computer facility (SUN grid), Philip Chan for helping me out immensely and facilitating to carry out my simulations. Mention must be made to Monash University Malaysia for providing me with the scholarship to pursue my PhD.

I would like to thank my closest friends Nishan and Hasuli who were pseudo-siblings for me from undergraduate level. Thank you for the support and encouragement. I would like to extend my thanks to Rangika and Devangi. Dr Anuja Dharmarathna, thank you for all the support, guidance and treating me as your own son when I needed help.

My Deepest gratitude goes out to my close friends in Monash Malaysia for helping me out, providing support and being there for me when I was going through very tough situations.

I am indebted for the support provided by my family. Amma, Thatha, Akki, Ayya and Sanula ("Johnny"). Amma thank you for firmly telling me that " A PhD has to be earned...!". A special thank goes out to Saranga for all the support you provided. My gratitude extends to Mr Nishantha Ranasinghe (Nishantha Ayya) for providing me strength and encouragement.

Last but definitely not least, I am much indebted to Mrs Malin Bamunuarachchi for the blessings, prayers and the encouragement given to me when I hit “rock-bottom” and was on the verge of giving up. Thank you madam.

# Dedication

*“ To Mrs. Malin Bamunuarachchi; whom without, this work would never have seen the light of day. Thank you madam; for your prayers, blessings, guidence, kind words of encourgaement and above all, believeing in me and giving me strength to get back up, when I myslef have given up hope....”*

# A list of publications related to this thesis


Jayatunga, H. G. K. G., Tan, B.T & Leontini, J.S. 2015 A study on the energy transfer of a square prism under fluid-elastic galloping *Journal of Fluids and Structures* **55**,384–397.

Leontini, J.S., Jisheng, Z., Jayatunga, H. G. K. G., Lo Jancono, D., Tan B. T., & Sheridan, J. 2014 Frequency selection and phase locking during aeroelastic galloping *19th Australasian Fluid Mechanics Conference, Melbourne, Australia*

# Nomenclature

| Symbol | Description |
|---|---|
| $a_1, a_3, a_5, a_7$ | Coefficients of the polynomial to determine $C_y$ |
| $A$ | Displacement amplitude |
| $c$ | Damping constant |
| $D$ | Characteristic length (side length) of the cross section of the body |
| $El$ | Subscript denoting integration over a single element |
| $f = \sqrt{k/m}/2\pi$ | Natural frequency of the system |
| $f_g$ | Frequency of galloping |
| $f_s$ | Frequency of vortex shedding |
| $f_{QSS}$ | Frequency predicted by the QSS model |
| $f_{lin}$ | Linear frequency |
| $f_{DNS}$ | Frequency predicted by DNS simulations |
| $F_y$ | Instantaneous force normal to the flow |
| $F_0$ | Amplitude of the oscillatory force due to vortex shedding |
| $\mathcal{F}$ | Fourier transform of velocity |
| $g$ | Index of the data points inside each element in the $\xi$-direction |
| $h$ | Variable indicative of resolution of macro-element mesh |
| $i$ | Index of the data point being considered during construction of the Lagrange polynomial in the $\xi$-direction |
| $\mathbf{J}$ | Jacobian operator for coordinate transformation |
| $j$ | Data point index in computational space in $\eta$-direction |

Continued on next page →

← Continued from previous page

| Symbol | Description |
|---|---|
| $k$ | Spring constant |
| $m$ | Mass of the body |
| $m_a$ | Added mass |
| $n$ | Timestep count to the current timestep |
| $\mathbf{n}$ | Unit vector in the normal direction to a boundary |
| $P_d$ | Power dissipated due to mechanical damping |
| $P_{in} = \rho U^3 D/2$ | Energy flux of the approaching flow |
| $P_m$ | Dimensionless mean power |
| $P_t$ | Power transferred to the body by the fluid |
| $P_s$ | Surface pressure |
| $P_{trial}$ | Trial solution for pressure |
| $q$ | Data point index in computational space in $\xi$-direction |
| $\mathbf{R}$ | Residual formed when substituting trial solution into governing equations |
| $s$ | Data point index in computational space in $\eta$-direction |
| $t$ | Time |
| $U$ | Freestream velocity |
| $U_i$ | Induced velocity |
| $V_m$ | velocity magnitude of the flow |
| $\mathbf{V}$ | Non-dimensional velocity vector, $\mathbf{u}/U$ |
| $\mathbf{V}_{trial}$ | Trial solution for velocity |
| $\mathbf{V}^*$ | Intermediate normalised velocity vector at the end of the advection sub-step |
| $\mathbf{V}^{**}$ | Intermediate normalised velocity vector at the end of the pressure sub-step |
| $\mathbf{V}_{cyl}$ | Transverse velocity of the cylinder, $\dot{y}/U$ |
| $\mathbf{V}_{cyl}^{(n+1)\dagger}$ | First approximation of $\mathbf{V}_{cyl}$ at the end of the timestep during the elastically-mounted cylinder convection substep |

Continued on next page →

← Continued from previous page

| Symbol | Description |
|---|---|
| $\mathbf{V}_{cyl}^{(n+1)\ddagger}$ | Second approximation of $\mathbf{V}_{cyl}$ at the end of the timestep during the elastically-mounted cylinder convection substep |
| $\mathbf{V}_{cyl}^{(n+1)\prime}$ | Approximation of $\mathbf{V}_{cyl}$ at the end of the timestep after relaxation during the elastically-mounted cylinder convection substep |
| $\mathbf{V}^{(n)}$ | Normalised velocity vector at timestep $n$ |
| $\mathbf{V}^{(n+1)}$ | Normalised velocity vector at timestep $n+1$ |
| $\widehat{\mathbf{V}^{*}}$ | Vector of $\mathbf{V}^{*}$ at the node points |
| $v$ | Normalised component of velocity in the $y$-direction |
| $\mathbf{v}_{cyl}$ | Instantaneous transverse cylinder velocity |
| $x$ | Cartesian coordinate in the freestream flow direction, positive downstream |
| $y$ | Cartesian coordinate transverse to the flow direction and span direction |
| $y_{cyl}$ | Transverse cylinder displacement |
| $y_{cyl}^{(n+1)\dagger}$ | A first approximation to $y_{cyl}$ at the end of the timestep during the elastically-mounted cylinder convection substep |
| $y, \dot{y}, \ddot{y}$ | Transverse displacement, velocity and acceleration of the body/cylinder |
| $\Delta\mathbf{V}_{cyl}$ | Change in $\mathbf{V}_{cyl}$ over one timestep |
| $\Delta\mathbf{V}_{cyl}^{\dagger}$ | First approximation of change in $\mathbf{V}_{cyl}$ over one timestep during the elastically-mounted cylinder convection substep |
| $\Delta\tau$ | The non-dimensional timestep |
| $\epsilon$ | Under-relaxation parameter used during the elastically-mounted cylinder convection substep |
| $\eta$ | Coordinate axis in computational space |
| $\xi$ | Coordinate axis in computational space |
| $\mathcal{A} = DL$ | Frontal area of the body |

Continued on next page →

← Continued from previous page

| **Symbol** | **Description** |
|---|---|
| $\lambda$ | Inverse time scale of a galloping dominated flow |
| $\lambda_{1,2}$ | Eigenvalues of linearised equation of motion |
| $\rho$ | Fluid density |
| $\omega_n = 2\pi f$ | Natural angular frequency of the system |
| $\omega_s$ | Vortex shedding angular frequency |
| $c^* = cD/mU$ | Non-dimensionalised damping factor |
| $C_y = F_y/0.5\rho U^2 DL$ | Normal (lift) force coefficient |
| $m^* = m/\rho D^2 L$ | Mass ratio |
| $Re$ | Reynolds number |
| $U^* = U/fD$ | Reduced velocity |
| $Y = y/D$ | Non-dimensional transverse displacement |
| $\dot{Y} = m^*\dot{y}/a_1 U$ | Non-dimensional transverse velocity |
| $\ddot{Y} = m^{*2} D\ddot{y}/a_1^2 U^2$ | Non-dimensional transverse acceleration |
| $\Gamma_1 = 4\pi^2 m^{*2}/U^{*2} a_1^2$ | First dimensionless group arising from linearised, |
| | Non-dimensionalised equation of motion |
| $\Gamma_2 = c^* m^*/a_1$ | Second dimensionless group arising from linearised, |
| | Non-dimensionalised equation of motion |
| $\zeta = c/2m\omega_n$ | Damping ratio |
| $\theta = \tan^{-1}(\dot{y}/U)$ | Instantaneous angle of incidence (angle of attack) |
| $\Pi_1 = 4\pi^2 m^{*2}/U^{*2}$ | Combined mass-stiffness parameter |
| $\Pi_2 = c^* m^*$ | Combined mass-damping parameter |

# Contents

# Chapter 1

# Introduction

The review of published literature reveals that fluid-elastic galloping has a potential to be used as a mechanism for energy extraction (Barrero-Gil et al., 2010). Thus, the following questions emerged. What are the optimum parameters for energy transfer in a galloping system? How do they influence galloping?

Over the years, VIV has been the popular research problem studied on flow induced vibrations. As a result, the parameters used to describe VIV problems (i.e $m^*$, $\zeta$ and $U^*$) have been incorporated to describe galloping, which could be observed throughout the current literature (Barrero-Gil et al., 2009, 2010; Parkinson and Smith, 1964).

However, mean power data presented using this classical VIV parameters (Barrero-Gil et al., 2010), does not provide a good collapse. A potential reason for this could be the difference in time scales of VIV and galloping.

Therefore, more relevant governing parameters for galloping could be obtained using the relevant time scales, from which, the optimum power output could be obtained. The work presented in this chapter is focused on testing this hypothesis.

Since the main mathematical model used to describe galloping is the Quasi-steady state model, the fluid-dynamic characteristics of flow over a static body are presented and discussed first. Then, the natural time scales of the system are obtained using the linearised QSS model. Next, the new non-dimensional governing parameters $\Pi_1$ and $\Pi_2$, are formulated by non-dimensionalising the QSS model from these natural time scales, followed by a comparison of galloping data using the classical VIV parameters and $\Pi_1$ and

$\Pi_2$. Then, the influence of $\Pi_1$ and $\Pi_2$ and the conditions for an optimum power output are discussed from QSS data. Finally, the QSS data are compared and discussed against FSI direct numerical simulations and final conclusions are presented.

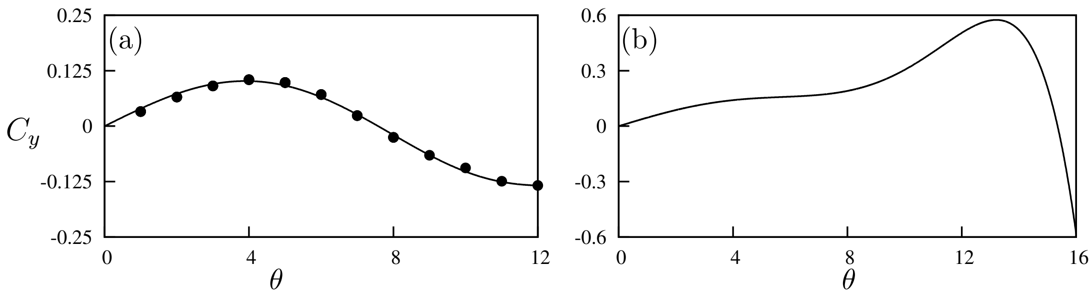


Figure 1.1: Lift coefficient, $C_y$, as a function of incidence angle $\theta$, for a static square cross section. (a) Data from simulations at $Re = 200$ and (b) data from Parkinson and Smith (1964) at $Re = 22300$. Points (•) are measurements from the simulations. Curves in both plots are 7th-order interpolating polynomials used to interpolate the fluid forcing for the QSS model.

### 1.0.1 Static body results

Since, the main data acquisition tool for galloping is the QSS model, the main input for this model, which is the interpolation forcing function based on the static body force coefficients data are presented here. As discussed in chapter QSS model uses an interpolation polynomial of the static body lift data as the driving force of the QSS equation. Figure 1.1 shows the plots $C_y$ as a function of $\theta$, as well as the interpolation polynomial curves. Data are acquired for high and low Reynolds numbers. For high Reynolds numbers, the static body polynomial data are obtained from Parkinson and Smith (1964) while for low Reynolds numbers a $7^{th}$ order non-linear least square regression fit on static body DNS simulations were used. The coefficients of these polynomials are presented in table 1.1.

There are several differences that can be observed between high and low Reynolds number data. The peak value of $C_y$ is significantly lower at $Re = 200$ ($C_y = 0.12$ at $5°$) compared to $Re = 22300$ ($C_y = 0.57$ at $13°$) . The inflection point present around $8°$ for $Re = 22300$ is not present at $Re = 200$. This agrees with the findings of Luo et al. (2003). It was concluded by Luo et al. (2003) that hysteresis in the system response occurs due to the inflection point in the $C_y$ curve. Therefore hysteresis is not expected at $Re = 200$.

The range of incident flow angles where $C_y$ remains positive is narrow at $Re = 200$ ($0° < \theta \leq 7°$) compared to $Re = 22300$ ($0° < \theta \leq 15°$). This feature is what sustains galloping. Power is only transferred from the fluid to the supporting structure within

| Case | $a_1$ | $a_3$ | $a_5$ | $a_7$ |
|---|---|---|---|---|
| $Re = 200$ | 2.32 | 197.8 | 4301.7 | 30311.9 |
| $Re = 22300$ | 2.69 | 168 | 1670 | 59900 |

Table 1.1: Coefficient values used in the 7th order interpolation polynomial for high ($Re = 22300$) and low ($Re = 200$) Reynolds numbers. These data are used as input data to calculate the right-hand side of Eq. **??** throughout this study.

this range of incident angles because fluid forces are acting in the direction of travel of, or in phase with, the oscillating body as demonstrated by equation **??**. Incident angles beyond this range actually suppress the galloping and power is transferred in the opposite direction, i.e; from body to fluid. Therefore due to the overall smaller $C_y$ and narrow range of angles where $C_y$ is positive for $Re = 200$ compared to $Re = 22300$, it is expected that the transferred power at $Re = 200$ is significantly lower than at $Re = 22300$.

# Bibliography

Alonso, G., Meseguer, J., Pérez-Grande, I., 2005. Galloping instabilities of two-dimensional triangular cross-section bodies. Experiments in Fluids 38, 789–795.

Alonso, G., Meseguer, J., Sanz-Andrés, A., Valero, E., 2010. On the galloping instability of two-dimensional bodies having elliptical cross-sections. Journal of Wind Engineering and Industrial Aerodynamics 38, 789–795.

Alonso, G., Valero, E., Meseguer, J., 2009. An analysis on the dependence on cross section geometry of galloping stability of two-dimensional bodies having either biconvex or rhomboidal cross sections. European Journal of Mechanics B/Fluids 28, 328–334.

Barrero-Gil, A., Alonso, G., Sanz-Andres, A., Jul. 2010. Energy harvesting from transverse galloping. Journal of Sound and Vibration 329 (14), 2873–2883.

Barrero-Gil, A., Sanz-Andrés, A., Roura, M., Oct. 2009. Transverse galloping at low Reynolds numbers. Journal of Fluids and Structures 25 (7), 1236–1242.

Bearman, P. W., Gartshore, I. S., Maull, D. J., Parkinson, G. V., 1987. Experiments on f low-induced vibration of a square-section cylinder. Journal of Fluids and Structures 1, 19–34.

Bernitsas, M. M., Ben-Simon, Y., Raghavan, K., Garcia, E. M. H., 2009. The VIVACE Converter: Model Tests at High Damping and Reynolds Number Around 10[sup 5]. Journal of Offshore Mechanics and Arctic Engineering 131 (1), 011102.

Bernitsas, M. M., Raghavan, K., Ben-Simon, Y., Garcia, E. M. H., 2008. VIVACE (Vortex Induced Vibration Aquatic Clean Energy): A new concept in generation of clean and renewable energy from fluid flow. Journal of Offshore Mechanics and Arctic Engineering 130 (4), 041101–15.

Blevins, R. D., 1990. Flow-Induced Vibration, 2nd Edition. New York: Van Nostrand Reinhold.

Bouclin, D. N., 1977. Hydroelastic oscillations of square cylinders. Master's thesis, University of British Columbia.

Den Hartog, J. P., 1956. Mechanical Vibrations. Dover Books on Engineering. Dover Publications.

Deniz, S. amd Staubli, T., 1997. Oscillating rectangular and octagonal profiles: Interaction of leading-and trailing-edge vortex formation. Journal of Fluids and Structures 11, 3–31.

Fletcher, C. A. J., 1984. Computational Galerkin methods. Springer-Verlag, New York.

Fletcher, C. A. J., 1991. Computational techniques for fluid dynamics. Vol. 1. Springer-Verlag, New York. Gabbai,.

Glauert, H., 1919. The rotation of an aerofoil about a fixed axis. Tech. rep., Advisory Committee on Aeronautics R and M 595. HMSO, London.

Griffith, M. D., Leontini, J. S., Thompson, M. C., Hourigan, K., 2011. Vortex shedding and three-dimensional behaviour of flow past a cylinder confined in a channel. Journal of Fluids and Structures 27 (5-6), 855–860.

Joly, A., Etienne, S., Pelletier, D., Jan. 2012. Galloping of square cylinders in cross-flow at low Reynolds numbers. Journal of Fluids and Structures 28, 232–243.

Karniadakis, G. E., Sherwin, S., 2005. Spectral/hp element methods for computational fluid dynamics, ii Edition. Oxford University.

Kreyszig, E., 2010. Advanced Engineering Mathematics, 10th Edition. John Wiley & Sons.

Lee, J., Bernitsas, M., Nov. 2011. High-damping, high-Reynolds VIV tests for energy harnessing using the VIVACE converter. Ocean Engineering 38 (16), 1697–1712.

Lee, J., Xiros, N., Bernitsas, M., Apr. 2011. Virtual damperspring system for VIV experiments and hydrokinetic energy conversion. Ocean Engineering 38 (5-6), 732–747.

Leontini, J. S., 2007. A numerical investigation of transversely-oscillating cylinders in two-dimensional flow. Ph.D. thesis, Monash University.

Leontini, J. S., Lo Jacono, D., Thompson, M. C., Nov. 2011. A numerical study of an inline oscillating cylinder in a free stream. Journal of Fluid Mechanics 688, 551–568.

Leontini, J. S., Thompson, M. C., 2013. Vortex-induced vibrations of a diamond cross-section: Sensitivity to corner sharpness. Journal of Fluids and Structures 39, 371–390.

Leontini, J. S., Thompson, M. C., Hourigan, K., Apr. 2007. Three-dimensional transition in the wake of a transversely oscillating cylinder. Journal of Fluid Mechanics 577, 79.

Luo, S., Chew, Y., Ng, Y., Aug. 2003. Hysteresis phenomenon in the galloping oscillation of a square cylinder. Journal of Fluids and Structures 18 (1), 103–118.

Luo, S. C., Yazdani, M., Chew, Y. T., Lee, T. S., 1994. Effects of incidence and afterbody shape on flow past bluff cylinders. Journal of Wind Engineering 53, 375–399.

Nakamura, Y., Mizota, T., 1975. Unsteady lifts and wakes of oscillating rectangular prisms. ASCE Journal of the Engineering Mechanics Division 101, 855–871.

Nakamura, Y., Tomonari, Y., 1977. Galloping of rectangular prisms in a smooth and in a turbulent flow. Journal of Sound and Vibration 52, 233–241.

Naudascher, E., Rockwell, D., 1994. Flow-induced vibrations: An engineering guide. A.A. Balkema, Rotterdam.

Naudascher, E., Wang, Y., 1993. Flow induced vibrations of prismatic bodies and grids of prisms. Journal of fluids and structures 7, 341–373.

Ng, Y., Luo, S., Chew, Y., Jan. 2005. On using high-order polynomial curve fits in the quasi-steady theory for square-cylinder galloping. Journal of Fluids and Structures 20 (1), 141–146.

Païdoussis, M., Price, S., de Langre, E., 2010. Fluid-Structure Interactions : Cross-Flow-Induced Instabilities. Cambridge University Press.

Parkinson, G., 1989. Phenomena and modelling of flow-induced vibrations of bluff bodies. Progress in Aerospace Sciences 26, 169–224.

Parkinson, G., Brooks, N. P. H., 1961. On the aeroelastic instability of bluff cylinders. Journal of Applied Mechanics 28, 252–258.

Parkinson, G. V., 1974. Mathematical models of flow-induced vibrations of bluff bodies. In Flow-Induced Structural Vibrations, e. naudascher Edition. Berlin: SpringerVerlag.

Parkinson, G. V., Smith, J. D., 1964. The square prism as an aeroelastic non-linear oscillator. The Quarterly Journal of Mechanics and Applied Mathematics 17 (2), 225–239.

Pregnalato, C., 2003. Flow-induced vibrations of a tethered sphere. Ph.D. thesis, Monash University.

Raghavan, K., Bernitsas, M., Apr. 2011. Experimental investigation of Reynolds number effect on vortex induced vibration of rigid circular cylinder on elastic supports. Ocean Engineering 38 (5-6), 719–731.

Raghavan, K., Bernitsas, M. M., Maroulis, D. E., 2009. Effect of Bottom Boundary on VIV for Energy Harnessing at $8 \times 10^3 < Re < 1.5 \times 10^5$. Journal of Offshore Mechanics and Arctic Engineering 131 (3), 031102.

Robertson, I., Li, L., Sherwin, S. J., Bearman, P. W., 2003. A numerical study of rotational and transverse galloping rectangular bodies. Journal of Fluids and Structures 17, 681 – 699.

Ruscheweyh, H., Hortmanns, M., Schnakenberg, C., 1996. Vortex-excited vibrations and galloping of slender elements. Journal of Wind Egineering and Industrial Aerodynamics 65, 347–352.

Sheard, G. J., Fitxgerald, M. J., Ryan, K., Jun. 2009. Cylinders with square cross-section: wake instabilities with incidence angle variation. Journal of Fluid Mechanics 630, 43.

Thompson, M., Hourigan, K., Sheridan, J., Feb. 1996. Three-dimensional instabilities in the wake of a circular cylinder. Experimental Thermal and Fluid Science 12 (2), 190–196.

Thompson, M. C., Hourigan, K., Cheung, A., Leweke, T., Nov. 2006. Hydrodynamics of a particle impact on a wall. Applied Mathematical Modelling 30 (11), 1356–1369.

Tong, X., Luo, S., Khoo, B., Oct. 2008. Transition phenomena in the wake of an inclined square cylinder. Journal of Fluids and Structures 24 (7), 994–1005.

Tu, J., Yeoh, G., Liu, C., 2008. Computational Fluid Dynamics: A Practical Approach, 1st Edition. Butterworth-Heinemann.

Vicente-Ludlam, D., Barrero-Gil, A., Velazquez, A., 2014. Optimal electromagnetic energy extraction from transverse galloping. Journal of Fluids and Structures 51, 281–291.

Vio, G., Dimitriadis, G., Cooper, J., Oct. 2007. Bifurcation analysis and limit cycle oscillation amplitude prediction methods applied to the aeroelastic galloping problem. Journal of Fluids and Structures 23 (7), 983–1011.

Weaver, D. S., Veljkovic, I., 2005. Vortex shedding and galloping of open semi-circular and parabolic cylinders in cross-flow. Journal of Fluids and Structures 21, 65–74.

White, F., 1999. Fluid mechanics, 4th Edition. McGraw-Hill, Boston.